

# Naval Research Laboratory

Washington, DC 20375-5000

DTIC FILE COPY



NRL Memorandum Report 5999

AD-A183 692

## Approaches to Resolving and Tracking Interfaces and Discontinuities

K. J. LASKEY\*, E. S. ORAN AND J. P. BORIS

*Laboratory for Computational Physics  
and Fluid Dynamics*

\**Berkley Research Associates, Inc.  
P.O. Box 852  
Springfield, VA 22150*

July 28, 1987

DTIC  
SELECTED  
AUG 21 1987  
S D  
GAD

87

8 14

Approved for public release; distribution unlimited.

SECURITY CLASSIFICATION OF THIS PAGE

HD-H183 692

## REPORT DOCUMENTATION PAGE

1a. REPORT SECURITY CLASSIFICATION UNCLASSIFIED		1b. RESTRICTIVE MARKINGS	
2a. SECURITY CLASSIFICATION AUTHORITY		3. DISTRIBUTION/AVAILABILITY OF REPORT Approved for public release; distribution unlimited.	
2b. DECLASSIFICATION/DOWNGRADING SCHEDULE			
4. PERFORMING ORGANIZATION REPORT NUMBER(S) NRL Memorandum Report 5999		5. MONITORING ORGANIZATION REPORT NUMBER(S)	
6a. NAME OF PERFORMING ORGANIZATION Naval Research Laboratory	6b. OFFICE SYMBOL (if applicable) Code 4040	7a. NAME OF MONITORING ORGANIZATION	
6c. ADDRESS (City, State, and ZIP Code) Washington, DC 20375-5000		7b. ADDRESS (City, State, and ZIP Code)	
8a. NAME OF FUNDING/SPONSORING ORGANIZATION Office of Naval Research	8b. OFFICE SYMBOL (if applicable)	9. PROCUREMENT INSTRUMENT IDENTIFICATION NUMBER	
8c. ADDRESS (City, State, and ZIP Code) Arlington, VA 22217		10. SOURCE OF FUNDING NUMBERS	
11. TITLE (Include Security Classification) Approaches to Resolving and Tracking Interfaces and Discontinuities			
12. PERSONAL AUTHOR(S) Laskey,* K.J., Oran, E.S. and Boris, J.P.			
13a. TYPE OF REPORT Interim	13b. TIME COVERED FROM _____ TO _____	14. DATE OF REPORT (Year, Month, Day) 1987 July 28	15. PAGE COUNT 31
16. SUPPLEMENTARY NOTATION *Berkley Research Associates, Inc., P.O. Box 852, Springfield, VA 22150			
17. COSATI CODES		18. SUBJECT TERMS (Continue on reverse if necessary and identify by block number) Interface tracking      Reactive flows	
FIELD	GROUP	SUB-GROUP	
19. ABSTRACT (Continue on reverse if necessary and identify by block number) → A review is presented of methods for modeling interfaces in numerical simulations. Interface capturing methods, in which the finest scales of the interface are resolved, and interface tracking approaches methods, in which the interface is treated as a discontinuity are discussed. Interface tracking approaches include moving-grid methods, surface-tracking methods, volume-tracking methods, and gradient methods. ←			
20. DISTRIBUTION/AVAILABILITY OF ABSTRACT <input checked="" type="checkbox"/> UNCLASSIFIED/UNLIMITED <input type="checkbox"/> SAME AS RPT. <input type="checkbox"/> DTIC USERS		21. ABSTRACT SECURITY CLASSIFICATION UNCLASSIFIED	
22a. NAME OF RESPONSIBLE INDIVIDUAL Elaine S. Oran		22b. TELEPHONE (Include Area Code) 202-767-2960	22c. OFFICE SYMBOL Code 4040

## CONTENTS

INTRODUCTION .....	1
RESOLVING INTERFACES .....	2
MOVING-GRID METHODS .....	3
SURFACE-TRACKING METHODS .....	5
VOLUME-TRACKING METHODS .....	7
THE GRADIENT METHOD .....	10
SUMMARY .....	13
REFERENCES .....	14

Accession For	
NTIS CRA&I	<input checked="" type="checkbox"/>
DTIC TAB	<input type="checkbox"/>
Unannounced	<input type="checkbox"/>
Justification .....	
By .....	
Distribution /	
Availability Codes	
Dist	Avail and/or Special
A1	



## APPROACHES TO RESOLVING AND TRACKING INTERFACES AND DISCONTINUITIES

### INTRODUCTION

In a numerical simulation, the interface between two different materials or different phases of the same material requires special consideration. There are two approaches to modeling the interface: interface capturing and interface tracking. Interface capturing involves resolving the finest scales of the physical processes controlling the interface. For example, to model the physics and chemistry at a flame front, the computation may have to resolve a structure less than 1 mm thick. The governing equations must contain terms to account for energy release due to chemical reactions, but these source terms are significant only in the region where the flame front resides. However, the same governing equations can be used throughout the computational domain and special modeling, other than possibly finer gridding, is not necessary in the vicinity of the front. The location of a finite thickness flame front is identified from the results of the calculations and is not known *a priori*. Interface capturing approaches are most often used when resolving the interface is the primary purpose of the calculation.

In a computation covering a large spatial domain, resolving a thin interface can be very expensive. For example, to model mixing and chemical reactions in a gas jet requires gridding fine enough to resolve the reaction front over a domain large enough to include the large-scale structures. But here the intent of the calculation is to determine the effects of reactions on the large-scale flow and not to investigate the details of the reaction fronts themselves. For such problems, the approach of interface tracking can be useful. The interface is represented as a discontinuity and a separate model is introduced to include the interface effects. This approach allows for a much coarser computational grid because the reaction front does not need to be resolved. To use interface tracking, the location of the interface must be determined prior to applying the interface tracking model. The numerical interface may be of zero or finite thickness, but the physical or chemical processes are not resolved even within the finite thickness numerical interfaces. The interfaces are advected and allowed to evolve separately from the surrounding medium. If the detailed structure of the physical interface is not necessary for a specific problem, and only the presence of the physical interface is important, then interface tracking provides a useful means of investigating large scale phenomena.

The following sections discuss both resolved physical interfaces and techniques for tracking numerical interfaces. Four major approaches for interface tracking are described. These are moving-grid methods, surface-tracking methods, volume-tracking methods, and gradient methods. Hyman (1984) reviews some of these, and Hirt and Nichols (1981) present a useful introduction.

## RESOLVING INTERFACES

The only way to capture an interface is to model the details of the controlling physical processes and to resolve the interface adequately. Sometimes the models we have are simply not good enough representations of the physical processes to be able to do this. When the models are sufficient, various grid refinement methods can be used to provide the necessary resolution. Here we give several examples of resolved, captured interfaces.

First, consider a laminar flame front moving through a mixture of hydrogen and oxygen gas, as shown in Figure 1 (Oran and Boris, 1981). The calculation includes models of the details of the chemistry, thermal conduction, molecular diffusion, and convection with enough resolution to simulate the detailed structure in the flame front. In such a calculation, it is necessary to model and calculate the individual processes very accurately in order to produce quantitatively correct values for the properties of the flame front. To do this, the calculation requires accurate input values for such quantities as chemical reaction rates and various diffusion coefficients. In this example, much more resolution is needed around the interface, here a flame front, than elsewhere in the system.

Next consider a calculation of a shock front propagating through a gas. The actual shock structure is on the scale of a few mean free paths, and is orders of magnitude too small to be resolved in a macroscopic fluid calculation. Nevertheless, most algorithms for simulating shocks are shock capturing algorithms. Numerical diffusion, flux limiters, or artificial viscosity play the role on the macroscopic scale that molecular viscosity plays on the microscopic scale. Generally at least a few cells are used to represent a relatively continuous shock profile. The shock is captured in the sense that the actual physical shock discontinuity is someplace near the middle of the gradient. The shock

is not modeled in the same detailed sense as the resolved flame front described above, and yet the conservation form of the equation generally ensures that the correct jump conditions across the shock are maintained. This global property of satisfying the jump conditions also ensures that shocks and contact surfaces move through or with the fluid at the correct local speed.

Another example of a resolved, captured interface is the calculation of the structure of a detonation front propagating in liquid nitromethane, shown in Figure 2 (Guirguis et al., 1987). This calculation was done with the two-dimensional compressible program based on the Flux-Corrected Transport algorithm (Boris and Book, 1976). The input to this model is a nitromethane equation of state and a model of the chemical reactions that includes measured chemical induction times and energy release times. Very fine resolution is required around the detonation front to calculate the complicated, interacting shock structure and the reaction zones that follow the leading shocks.

The final example of a captured interface is an ablation layer caused by the deposition of laser energy on a solid target. One such calculation is shown in Figure 3, taken from the work of Emery et al. (1982). The interface is the receding surface of the solid target, on the left of the two calculations shown. As energy from the laser is deposited on the surface of the target, a high-pressure plasma layer is formed. The surface of the target is unstable to the Rayleigh-Taylor instability as a result of this low-density, high-pressure layer. We generally think of this instability in terms of a heavy fluid sitting on top of a light fluid in the presence of gravity. These calculations were done with a two-dimensional Flux-Corrected Transport program similar to the program that calculated the two-dimensional detonation just described. The difference here is that there are now algorithms included for strong electron thermal conduction and inverse bremsstrahlung. The two panels show the nonlinear evolution of two different wavelength perturbations at the interface.

## MOVING-GRID METHODS

Moving-grid methods define the grid so that the interface is always located on cell boundaries. Maintaining a cell boundary between different fluids controls numerical smearing that can occur at the interface as the fluid is transported. The interface is

then a well defined continuous curve because it coincides with cell boundaries. There are several approaches to actually implementing this idea. One is to maintain a grid of distorted quadrilaterals (Hyman and Larroutuou, 1982). Another approach is to use generalized orthogonal grids that fit the form of the interface. And yet another is to use a Lagrangian representation with triangular cells (Fritts and Boris, 1979). We might also try a combination methods that use a limited Lagrangian grid to represent the interface as it moves through a rectangular Eulerian grid on which the overall fluid problem is solved (Noh, 1964).

All of these approaches have advantages and disadvantages. The common advantages are obvious: a potentially good representation of the interface. Using a quadrilateral moving grid can cause problems, however, when there are motions in the flow that severely distort the grid, as shown in Figure 4. One remedy requires defining a new grid and interpolating the physical variable onto that grid. This interpolation introduces numerical diffusion into the calculation. Some of the triangular grid approaches do not have this problem, but instead have significant bookkeeping problems and hefty computer storage requirements.

A combination of both an Eulerian grid and a superimposed Lagrangian grid tries to have the versatility of representing the interface on an adaptable grid and still keep the convenient features of a rectangular grid for the fluid dynamics. In the CEL program (Noh, 1964), a series of straight-line segments represents the interface. For example, an isolated pocket of fluid would be bounded by an irregular polygon. The calculation for one timestep proceeds in several steps. First, the Lagrangian grids defining interfaces are advected through the Eulerian domain. Then, the calculations for the various fluids are done on the Eulerian grid using the newly calculated Lagrangian positions of the interface. Finally the velocity and pressure fields from the Eulerian calculation are used to calculate the Lagrangian positions at the start of the next timestep. An initial CEL gridding for a sample problem with a number of interfaces is shown in Figure 5. Although methods such as CEL isolate the various fluids from each other, the problem of distorting Lagrangian grids is still present. In addition, this method requires storing information for both the Eulerian and Lagrangian grids, as well as rather expensive logic and computation to interpolate back and forth between the two grids.

A fully Lagrangian method seems like the most natural way to track many interfaces. Fritts and Boris (1979) introduced the Lagrangian triangular grid designed to avoid problems related to rectangular cells. When space is divided into quadrilateral cells, the connectivity of grid points is inflexible: each vertex is common to four quadrilaterals. When we divide space into triangles, a vertex may be common to any number of triangles. Thus the distortion problem can be avoided by locally restructuring the grid. For example, an elongated cell arising from shear flow in the fluid can be replaced by one that is more symmetric, as shown in Figure 6.

Figure 7 shows a calculation of the Rayleigh-Taylor instability at the interface between two fluids using the Lagrangian algorithm of Fritts and Boris. The initial configuration is a heavy fluid on top of a light fluid in the presence of a vertical gravitational field. Given a small perturbation at the interface between the fluids, the interface is unstable and the heavy fluid tends to penetrate the light fluid as it falls. By the last panel in the figure, the heavy fluid has penetrated the light fluid significantly and mixing is well underway. A number of new cells have been added to keep the interface well resolved as it rolls up and there are now isolated pieces of one fluid mixed within the other. The interface between fluids is a series of connected triangle sides, so that the border is composed of pieces of straight lines. The resolution of the interface is limited by the minimum length permitted for a triangle side and the representation of the physical boundary by straight line segments. But within these constraints, the interface is tracked quite well.

## SURFACE-TRACKING METHODS

Surface-tracking methods represent an interface as a connected series of interpolated curves through points on the interface. At each timestep, the points are saved in an array along with the information about the sequence in which they are connected. These points are advected with the flow field. The points can also be moved to simulate processes other than convection, such as chemical reactions, phase changes, or ablation. The surface-tracking methods have been used by Glimm et al. (1983) and Chern et al. (1986). We note that the contour dynamics methods (Zabusky, et. al., 1979) for solving certain types of fluid problems has many of the features of the surface-tracking algorithms described here.

In the simplest forms of surface-tracking methods for two dimensions, the points are saved as a sequence of heights above a given reference line, as shown in Figure 8a. Two curves are shown bounding the top and the bottom of a region of fluid. This approach fails if the interpolated curve is multivalued or does not extend all the way across the region. However, this problem may be avoided if the points follow a parametric representation, such as that shown in Figure 8b. The parametric formulation is more complex, but it can represent fine detail in the interface if enough points are used. An interesting feature of these methods is that they can resolve features of the interface that are smaller than the cell spacing of the macroscopic Eulerian grid on which the curves are overlaid. There is naturally a price paid for storing this additional information. The timestep for the entire calculation can be limited by the amount of movement the interface can undergo during each timestep.

There are still two major problems. First, it is very difficult to handle merging interfaces or joining a part of an interface to itself. This requires re-ordering the interface points, which could require significant computational bookkeeping, and possibly tracking additional interfaces. Second, for a given problem, the points can accumulate in one segment of the interface leaving other segments without enough resolution. For the most accuracy, it is best to limit the largest distance between neighboring points to be something less than the minimum size of the local computation grid (Hirt and Nichols, 1981). Interface areas typically increase continually in complex flows. Thus it is necessary to add points along the interface automatically. Conversely, points should be deleted where there are too many. When points must be added or deleted, the best way to interpolate new points and the best way to represent and manipulate contours with changing lengths are major computational issues.

Development of surface-tracking methods continues, but the problems of changing topology from simply connected to multiply connected regions, merging fronts, disappearance of weakened fronts, and the appearance of new fronts have yet to be solved. The methods have generally been used in one- and two-dimensional calculations for interfaces that do not interact. The complexity in specifying an interface and treating three-dimensional interactions may limit applications of surface tracking in three dimensions.

## VOLUME-TRACKING METHODS

Unlike the surface-tracking methods that store a representation of the interface, volume-tracking methods reconstruct the interface whenever it is needed. The reconstruction is done cell by cell and is based on the presence of a marker quantity within the cell. Whereas the surface-tracking methods represent the interface by a continuous curve, the interface generated by volume tracking consists of a set of disconnected segments from the cells containing parts of the interface.

The earliest volume-tracking methods used marker particles so that the density of particles in each cell indicates the density of the material. This method was first proposed by Harlow (1955) and was called the Particle-in-Cell or PIC method. In the Marker-and-Cell or MAC method (Harlow and Welch, 1965; Welch et al., 1966), the particles are tracers, marker particles with no mass.

As an example, we consider some of the features of the PIC method implemented by Amsden (1966). PIC uses an Eulerian grid in which velocity, internal energy, and total cell mass are defined at cell centers. In addition, the different fluids are represented by Lagrangian mass points, the marker particles, that move through the Eulerian grid. The marker particles each have a constant mass, a specific internal energy, and a recorded location in the Eulerian grid, and are moved with a local velocity. The particle mass, momentum, and specific internal energy are transported from one cell to its neighbor when the marker particle crosses the cell boundary. Cells containing marker particles of both fluids contain the interface. Since the interface can be reconstructed locally at any time, the problems associated with interacting interfaces and large fluid distortions are eliminated. The method generalizes to any number of fluids.

Unlike the surface-tracking methods, marker-particle methods cannot resolve details of the interface which are smaller than the mesh size. However, the methods are still expensive with respect to their requirements in computer time and memory. As with the surface-tracking methods, particles may accumulate in portions of the grid, thus leaving other portions not well enough resolved. Since mass, momentum, and energy are associated with each particle in the PIC method, addition and deletion of

particles is not that straightforward. Unacceptable statistical fluctuations arise when there are not enough marker particles and when the local variation of the attributes of the marker particles is too large.

Many of the volume-tracking methods use the fraction of a cell volume occupied by one of the materials as the marker for reconstructing the interface. If this fraction is zero for a given cell, the material does not occupy the cell and there is no interface in that cell. Conversely, if the fraction is one, the cell is completely occupied by the material and again there is no interface present. An interface is constructed only if the fractional marker volume is between zero and one.

The Simple Line Interface Calculation (SLIC) algorithms were first proposed by Noh and Woodward (1976). Each grid cell is partitioned by a horizontal or vertical line such that the volume of the partitioned part of the cell equals the fractional marker volume. The orientation of the line is chosen so that as to keep similar types of fluid in neighboring cells adjacent. Thus a preference is given for lines through cells that are normal to the direction of flow. Given a cell with an interface separating two fluids, if the contents of this cell flows into an adjacent cell containing only one of the fluids, then an interface orientation normal to the flow direction causes all of the common fluid to move across the cell boundary before the second fluid enters the initially single-fluid adjacent cell. This minimizes numerical diffusion between cells. The method assumes timestep splitting is used in multidimensional problems, so that extensions to two or three dimensions are straightforward. For the two-dimensional case, the interface is constructed cell by cell before advection in the  $x$ -integration. After the  $x$ -integration, the interface is reconstructed and the  $y$ -integration is done. Line segments normal to the direction of flow usually result in different representations of the interface for the  $x$ - and  $y$ -sweeps. To avoid such a directional bias, the order of  $x$ - and  $y$ -integrations is changed every timestep. Samples of SLIC interface approximations are shown in Figures 9 and 10.

Chorin (1980) improved the resolution of the original SLIC algorithm by adding a corner interface to the straight horizontal and vertical lines used by Noh and Woodward, but still using the same fractional cell volume as the variable for locating the interface. An example of this SLIC interface is shown in Figure 11b. Chorin used the vortex

dynamics method to calculate the vorticity field. The vorticity gives the velocity field and these velocities are used to advect the interface. Advection is done in the same time-split manner as for the original SLIC algorithm.

To simulate the evolution of the interface, in particular, flame propagation, Chorin uses an idea based on Huygens' principle. Given a number of different directions, the interface is propagated at a known speed in each of the directions separately and the effect on the volume fractions for each propagation direction is stored. The final interface position is the position that assigns the largest increase in the burned volume to each cell. Chorin chose eight directions at angles  $\alpha_l = (l - 1)\pi/4$ ,  $l = 1, \dots, 8$ . Each propagation was carried out using the same timestep-splitting process as for the advection. In the straightforward application of this idea, it is possible for interfaces which initially start out as circles to evolve into octagons. Such problems are due to preferential propagation in the eight directions. They may be avoided in several ways, for example, by using random starting angles. This interface construction, advection, and propagation sequence appears in combustion studies by Ghoniem et al. (1981, 1986) and Sethian (1984).

The VOF method of Hirt and Nichols (1981) also represents the interface within a cell by a straight line, but the line may have any slope. A numerical estimate of the  $x$ -direction and  $y$ -direction derivatives of the volume of fluid occupying a cell are obtained for a given cell. If the magnitude of the  $x$ -direction derivative is smaller than the magnitude of the  $y$ -direction derivative, then the interface is more nearly horizontal and its slope is the value of the  $x$ -direction derivative. A more vertical interface has a slope equal to the value of the  $y$ -direction derivative. If the  $x$ -direction derivative represents the slope of the interface, then the sign of the  $y$ -direction derivative determines whether the fluid is above (positive) or below (negative) the interface. For a more vertical line, the sign of the  $x$ -direction derivative identifies the location of the marker fluid to the right (positive) or the left (negative) of the interface. Thus, given the slope of the interface and the side of the interface on which the fluid is located, the position of the interface within the cell is set. This process is done for every cell with an occupied volume between zero and one. Hirt and Nichols use values of the fractional volume of fluid averaged over several cells to calculate the derivatives. Other

implementations of VOF use a simple central difference (Barr and Ashurst, 1984).

The VOF method depends on the ability to advect the volume fraction through the grid accurately without smearing from numerical diffusion. Hirt and Nichols have described a "donor-acceptor" method to insure that only the appropriate constituent fluid moves to or from a cell containing an interface. This helps to avoid cell averaging that results in numerical diffusion.

To analyze combustion problems, Barr and Ashurst (1984) use both VOF and the Chorin version of SLIC in a method called SLIC-VOF. The SLIC algorithm is used to define and advect interfaces and VOF is used to define the normal direction and to give a smoother interface for the flame propagation phase. Figure 11 shows how SLIC and VOF approximate the same curved interface. For a two-dimensional flame propagation problem, SLIC-VOF performs the  $x$  integration of the SLIC interface, the  $y$  integration of the SLIC interface, the  $x$ -direction flame propagation of the VOF interface, and then the  $y$ -direction flame propagation of the VOF interface. The interfaces are reconstructed following each advection or propagation calculation. At each timestep, the order of the  $x$ - and  $y$ -sweeps are interchanged, but convection always precedes burning. As in the Chorin implementation, flow velocities are calculated from a vorticity field. The flame propagation speed in the  $x$ - and  $y$ -directions is the respective vector component of a velocity vector normal to the interface defined by VOF with the magnitude of the specified flame speed.

Barr and Ashurst (1984) give a detailed discussion of the problems with SLIC algorithms. In brief, curved surfaces may be flattened or even indented. This distortion depends on the Courant number of the flow and the interface geometry. In some cases this distortion appears as the interface first moves across a cell and does not increase thereafter. In other cases the distortion continues to grow. Including a model for propagating chemical reactions apparently decreases this distortion since the propagation step smooths short-wavelength wrinkles.

## THE GRADIENT METHOD

The gradient method (Laskey et al., 1987) does not attempt to define the exact location of the interface within a cell, but it represents the interface as a relatively

continuous gradient over several cells. By keeping the resolution of the interface at the limit of that of the numerical convection algorithm, the amount of surplus computer storage requirements and the cost of interface tracking can be reduced. Laskey has applied this method to flame fronts, although it may also be useful for other types of interfaces. We briefly describe some of the elements of the flame front tracking problem because of its importance in reactive flows.

A system of gases react to form a product whose number density is  $n_p$ . We solve an equation of the form

$$\frac{\partial n_p}{\partial t} + \nabla \cdot n_p \vec{v} = w, \quad (11 - 2.1)$$

where  $n_p$  is the number density of product and the right hand side is the production term. The left hand side can be solved by any method for solving continuity equations. The production term is added to the solution of the convection by timestep-splitting methods. Conservation among the reactants and the product determines the amount of energy released in each cell.

In this method, the reaction fronts are identified by the region in which there is a large gradient, that is, where  $\nabla n_p$  is large. The integral of the gradient from the front to the back of the extended interface is known. This is used to define a local energy release rate and tends to guarantee the correct overall energy release along the convoluted front. The gradient is assumed to be the result of the presence of the reaction front, and thus, the amount of new product formed is

$$\Delta n_p = |\nabla n_p|l, \quad (11 - 2.2)$$

where  $\Delta n_p$  is the change in  $n_p$  and  $l$  is the distance the front moves normal to itself locally during the time interval of interest. The direction of the normal to the reaction front is the same as the direction of the gradient. The speed of the front is the local burning velocity. Therefore  $l$  is approximated by

$$l = v_b \Delta t. \quad (11 - 2.3)$$

where  $v_b$  is the local flame speed normal to the interface. The amount of product formed per unit volume in the time interval  $\Delta t$  is

$$w \equiv \Delta n_p = v_b \Delta t |\nabla n_p|. \quad (11 - 2.4)$$

The calculation requires determining  $|\nabla n_p|$ . Laskey et al. (1987) have found that the one-sided difference approach for evaluating the gradient, although technically only first-order accurate, gives better results than a second-order central difference. In addition, there are several tests which must be made on the gradient to determine if the numerical estimate of the gradient is a valid quantity. Finally, some modification is required for the case of a nonuniform temperature field. The burning velocity  $v_b$  becomes a function of position and the number densities considered must be scaled to a reference temperature. An example of a gradient method calculation of two round flame fronts that grow and merge is shown in Figure 12.

There are several good features of the gradient method. It ensures that the right amount of reaction takes place in the vicinity of the gradient, as defined by the macroscopic grid. Also, it treats the effects of merging interfaces with relatively little difficulty. Adding other interface processes, and eventually ignoring weakened interfaces results naturally from the formulation. Because no additional variables are needed, computer memory requirements are modest. The algorithm as implemented is fully vectorized. Finally, it is straightforward to extend the two-dimensional formulation to three dimensions.

There are several drawbacks to the gradient method. As with the volume tracking methods, the location of the reaction front is only approximately known. Thus, if it is necessary to track the curvature at the surface on scales comparable or smaller than the Eulerian grid spacing, another method should be used. An example of a problem for which the gradient method is not suited is the dynamics of a droplet in which it is important to know the curvature of a surface very accurately for calculating the effects of surface tension. (see, for example, Fyfe et al., 1987).

Probably the most important limitation is that the gradient method assumes the largest gradients appearing within the computational domain are located at the interface and are the direct result of the existence of the interface. If large gradients exist apart from the interface, then the gradient method may not be appropriate. An analogous problem can plague any interface-tracking method which reconstructs the interface using some quantity which should be indicative of the interface. If this quantity is contaminated, spurious interfaces may result.

An important requirement of the gradient method is the gradients that the method tries to represent remain quite large. This requires an advection algorithm which minimizes numerical diffusion of the quantity used to define the interface. For this purpose the present implementation of the gradient method is used in conjunction with a high-order nonlinear monotone methods, such as Flux-Corrected Transport.

## SUMMARY

A review has been presented of various approaches to modeling interfaces in numerical simulations. Interface capturing methods attempt to resolve the details of the structure of the interface and are most useful when the interface structure is crucial to the calculation. However, numerically capturing an interface requires fine gridding on the scale of the structure and very accurate values for input physical properties. If it is not necessary to resolve the detailed structure of the interface, then the interface can be treated as a discontinuity and interface tracking is useful.

There are several types of interface tracking methods. Surface-tracking methods track discrete points on the interface while volume-tracking methods use a marker quantity to reconstruct the interface when it is needed. Moving-grid methods alter the computational grid so that the interface is always along cell boundaries. In all these interface tracking methods, an exact location of the interface is defined prior to calculating the interface effects. The gradient method differs from these in that the effect of the interface is calculated without defining the interface location; the location can be reconstructed for diagnostic purposes after the calculation is complete. Like the volume-tracking methods, the calculation for the gradient method is based on a marker quantity carried with the flow.

All of these methods are idiosyncratic. They work best under a specific set of conditions, and are not totally general purpose. Therefore, the various strengths and limitations of each of the interface tracking methods makes the choice of method dependent on the problem at hand.

## REFERENCES

Amsden, A.A., 1966, *The Particle-in-Cell Method for the Calculation of the Dynamics of Compressible Fluids*, LA-3466, Los Alamos Scientific Laboratory, Los Alamos, New Mexico.

Barr, P.K., and W.T. Ashurst, 1984, *An Interface Scheme for Turbulent Flame Propagation*, SAND82-8773, Sandia National Laboratory, Livermore, CA.

Boris, J.P., and D.L. Book, 1976, Solution of Continuity Equations by the Method of Flux-Corrected Transport, *Methods in Computational Physics*, vol. 16, pp. 85-129.

Chern, I-L., J. Glimm, O. McBryan, B. Plohr, and S. Yaniv, 1986, Front Tracking for Gas Dynamics, *J. Comp. Phys.* 62: 83-110.

Chorin, A.J., 1980, Flame Advection and Propagation Algorithms, *J. Comp. Phys.* 35: 1-11.

Chorin, A.J., 1985, Curvature and Solidification, *J. Comp. Phys.* 57: 472-490.

Emery, M.H., J.H. Gardner, and J.P. Boris, 1982, Nonlinear Aspects of Hydrodynamic Instabilities in Laser Ablation, *Appl. Phys. Letters* 41: 808-810.

Fyfe, D., E.S. Oran, and M.J. Fritts, 1987, to appear in *J. Comp. Phys.*.

Glimm, J., B. Lindquist, O. McBryan, B. Plohr, and S. Yaniv, 1983, Front Tracking for Petroleum Reservoir Simulation, *Proceedings of the Seventh SPE Symposium on Petroleum Reservoir Simulation*, SPE-12238, pp. 41-49, Society of Petroleum Engineers, Dallas.

Ghoniem, A.F., A.J. Chorin, and A.K. Oppenheim, 1981, Numerical Modeling of Turbulent Combustion in Premixed Gases, *Eighteenth Symposium (International) on Symposium on Combustion*, The Combustion Institute, Pittsburgh, PA, pp. 1375-1383.

Ghoniem, A.F., D.Y. Chen, and A.K. Oppenheim, 1986, Formation and Inflammation of a Turbulent Jet, *AIAA J.* 24, 224-229.

Guirguis, R., E.S. Oran, and K. Kailasanath, 1986, Numerical Simulations of the Cellular Structure of Detonations in Liquid Nitromethane - Regularity of the Cell Structure, to appear in *Comb. Flame*.

Harlow, F.H., 1955, *A Machine Calculation Method for Hydrodynamic Problems*. LAMS-1956, Los Alamos Scientific Laboratory, Los Alamos, New Mexico.

Harlow, F.H., and J.F. Welch, 1965, Numerical Calculation of Time-Dependent Viscous

Incompressible Flow of Fluid with Free Surface, *Phys. Fluids* 8: 2182-2189.

Hirt, C.W., and B.D. Nichols, 1981, Volume of Fluid (VOF) Method for the Dynamics of Free Boundaries, *J. Comp. Phys.* 39: 201-225.

Hyman, J.M., 1984, Numerical Methods for Tracking Interfaces, *Physica* 12D: 396-407.

Hyman, J.M., and B. Larrouturou, 1982, The Numerical Differentiation of Discrete Functions Using Polynomial Interpolation Methods, *Appl. Math. and Comp.*, vols. 10-11, pp. 487-506.

Laskey, K.J., E.S. Oran, and J.P. Boris, 1987, The Gradient Method for Interfacing Tracking, to appear in *J. Comp. Phys.*.

Noh, W.F., and P. Woodward, SLIC (Simple Line Interface Method), 1976, *Proceedings of the Fifth International Conference on Numerical Methods in Fluid Dynamics*, in A.I. van de Vooren and P.J. Zandbergen, eds., *Lecture Notes in Physics*, vol. 59, pp. 330-340, Springer-Verlag, New York.

Noh, W.F., 1964, CEL: A Time-Dependent, Two-Space-Dimensional, Coupled Eulerian-Lagrange Code, in B. Adler, S. Fernbach, and M. Rotenberg, eds., *Methods in Computational Physics*, vol. 3, pp. 117-179.

Oran, E.S., and J.P. Boris, 1981, Theoretical and Computational Approach to Modeling Flame Ignition, in J.R. Bowen, N. Manson, A.K. Oppenheim, and R.I. Soloukhim, eds., *Combustion in Reactive Systems*, Vo. 76, *Progress in Astronautics and Aeronautics*, pp. 154-171, AIAA, New York.

Sethian, J., 1984, Turbulent Combustion in Open and Closed Vessels, *J. Comp. Phys.* 54: 425-452.

Welch, J.E., F.H. Harlow, J.P. Shannon, and B.J. Daly, 1966, *The MAC Method: A Computing Technique for Solving Viscous, Incompressible, Transient Fluid Flow Problems Involving Free Surfaces*, LA-3425, Los Alamos Scientific Laboratory, Los Alamos, New Mexico.

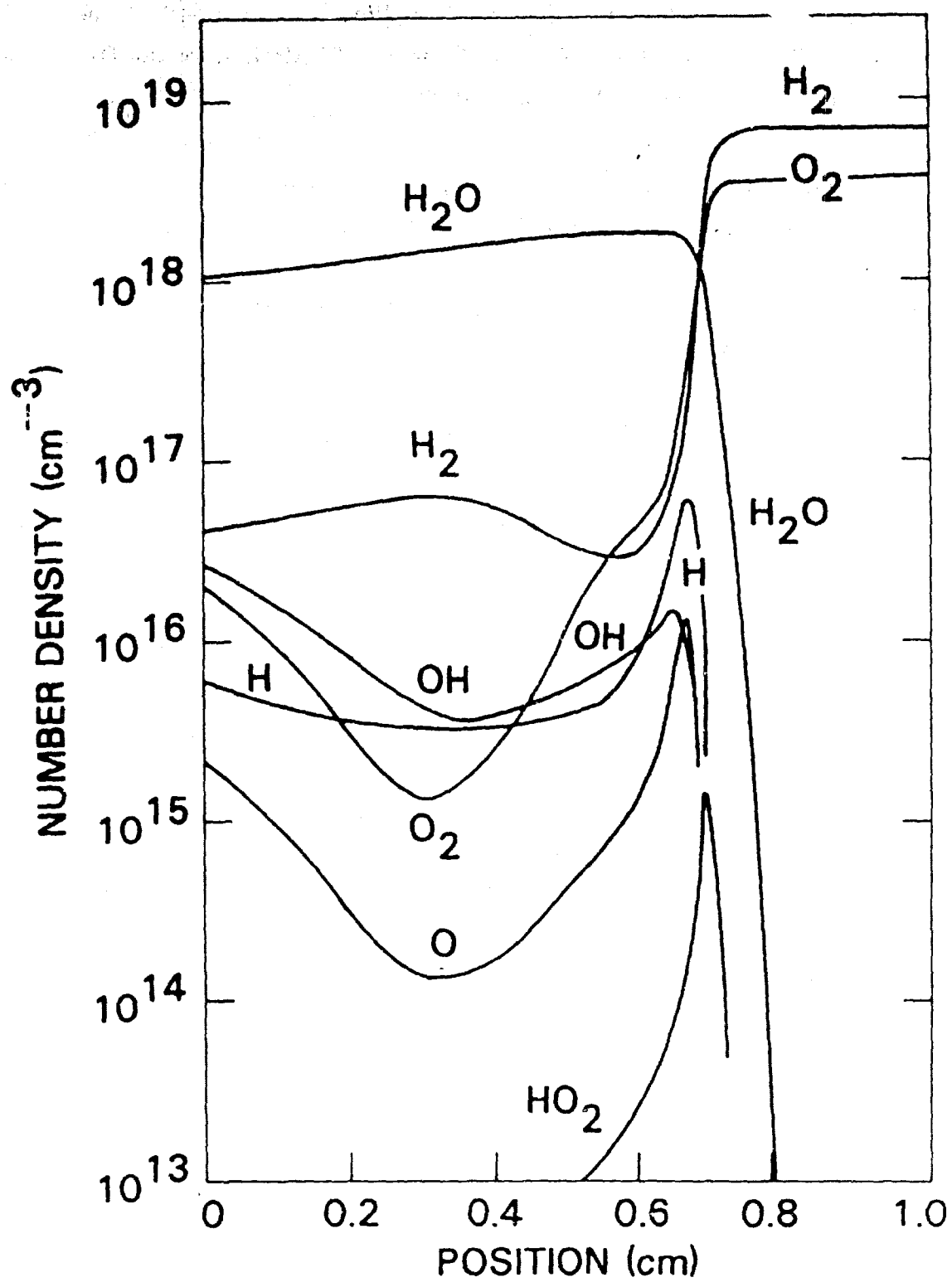


Figure 1. Calculation of the chemical structure of a flame propagating in a mixture of hydrogen and oxygen (Oran and Boris, 1981.)

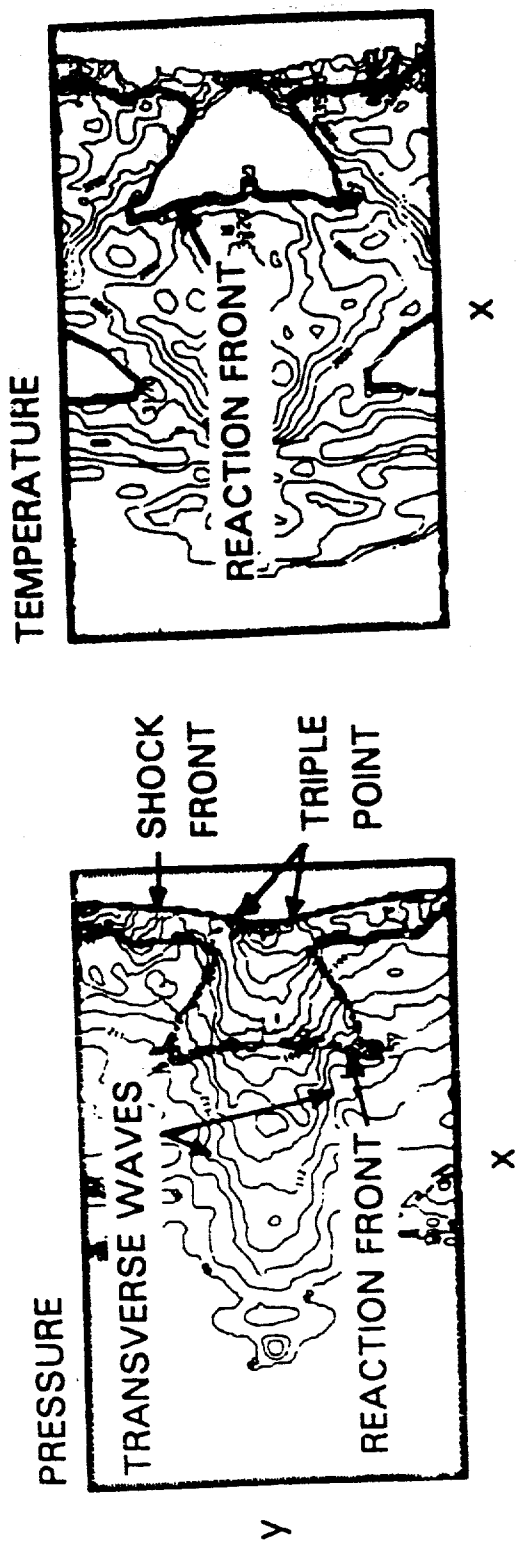


Figure 2. Temperature and Pressure profiles for a two-dimensional calculations of a detonation propagating in liquid nitromethane (Guirguis et al., 1986.)

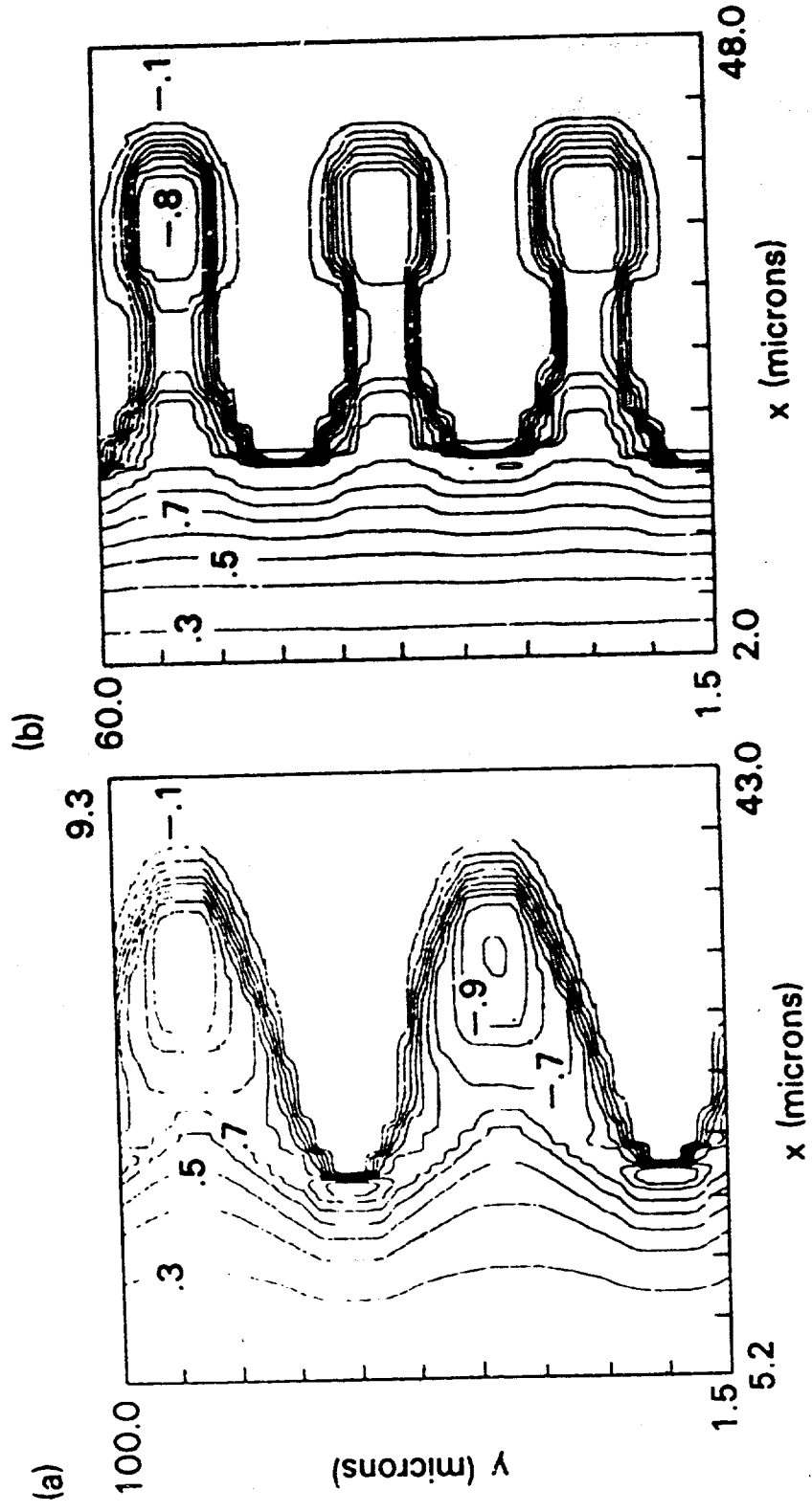


Figure 3. Calculation of a the ablation of material from a plastic target irradiated by a laser. The Rayleigh-Taylor instability is initiated by small density perturbation at the surface. The figures show the results of two different wavelength perturbations along the surface. (Emery et al., 1982.)

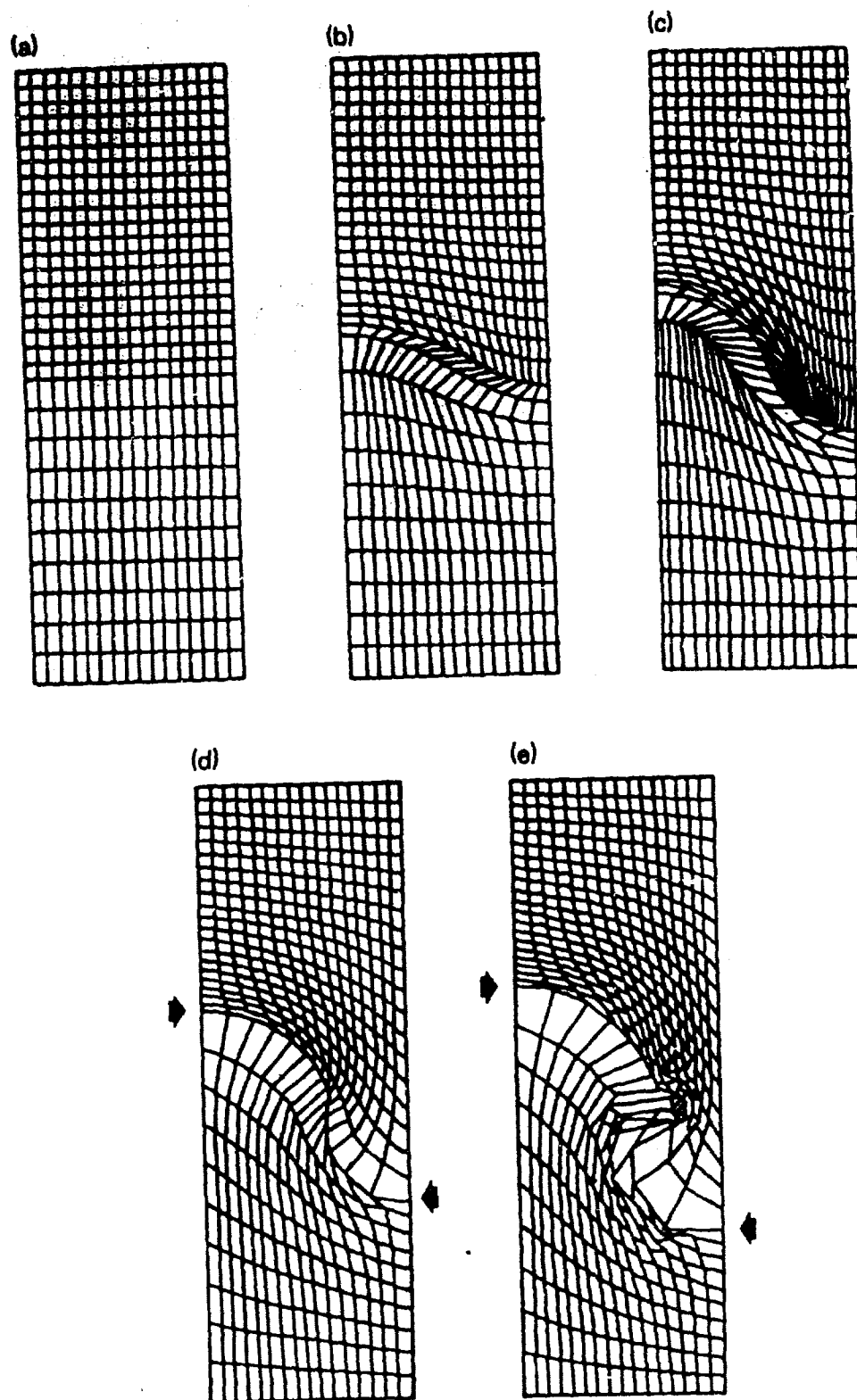


Figure 4. A Lagrangian calculation of a Rayleigh-Taylor instability with quadrilateral cells. The arrows indicate the location of the interface on each side of the figures. A heavy fluid is on top of the light fluid, and the effects of gravity are included. A small perturbation at the interface at the beginning of the calculation initiates the instability. By (b), the calculation cannot proceed because grid lines have crossed. Regridding is then necessary. (Figure courtesy of M. Fritts.)

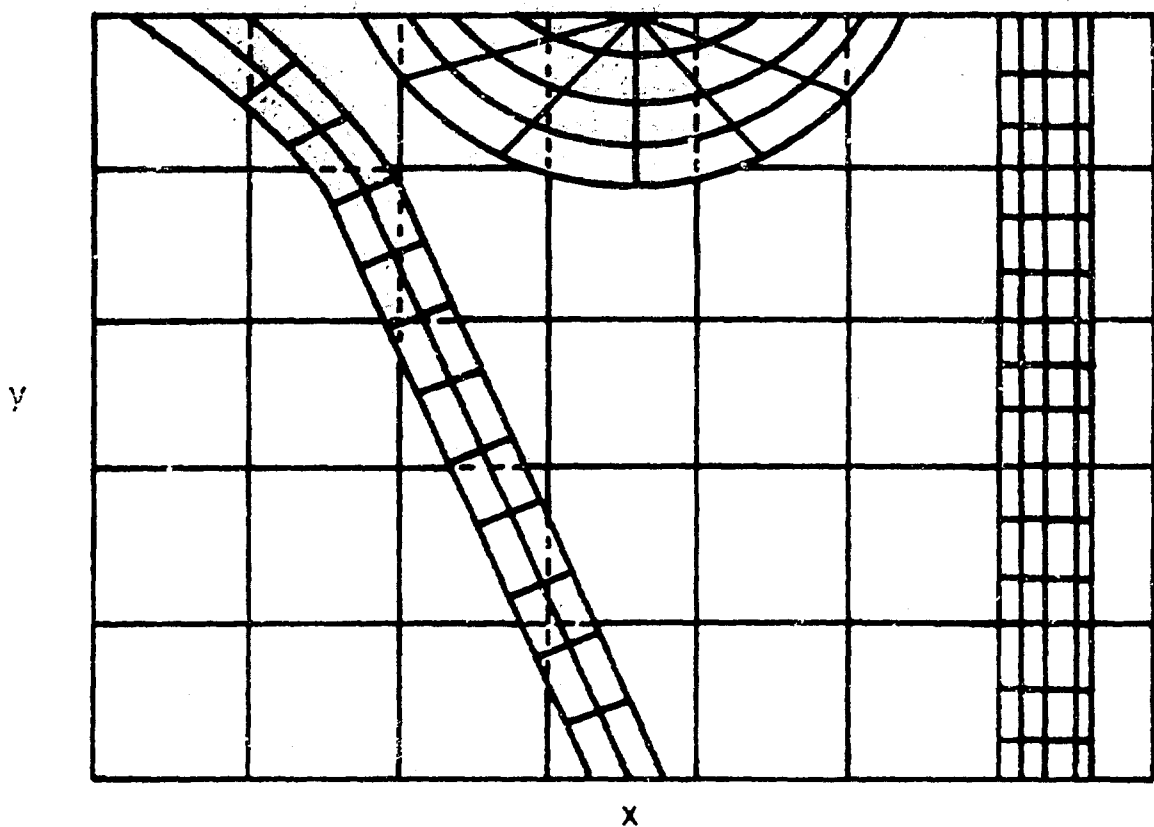


Figure 5. A possible initialization for a problem with multiple interfaces using the CEL method. (Figure courtesy of W. Noh.)

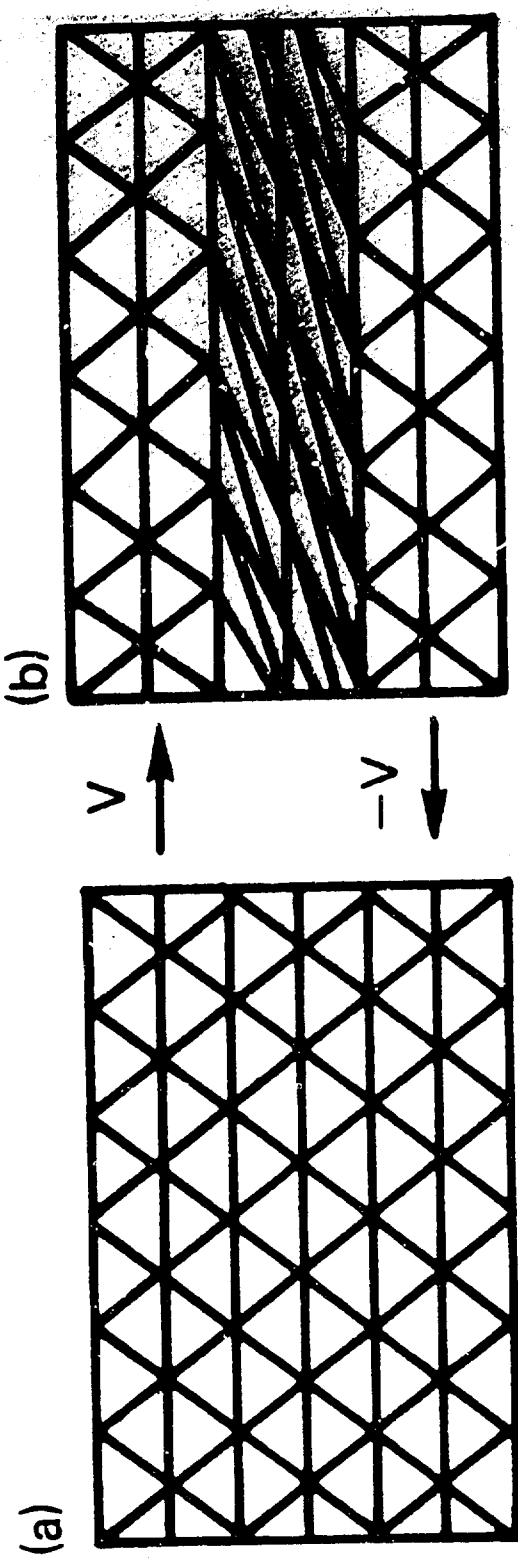


Figure 6. The initial conditions for a shear flow calculation using a Lagrangian triangular grid are shown in (a). The velocity of the upper fluid is  $v$ , and the lower fluid is  $-v$ . After some time, the grid can distort, as shown in (b). Then the grid vertices can be reconnected again to produce the grid (a).

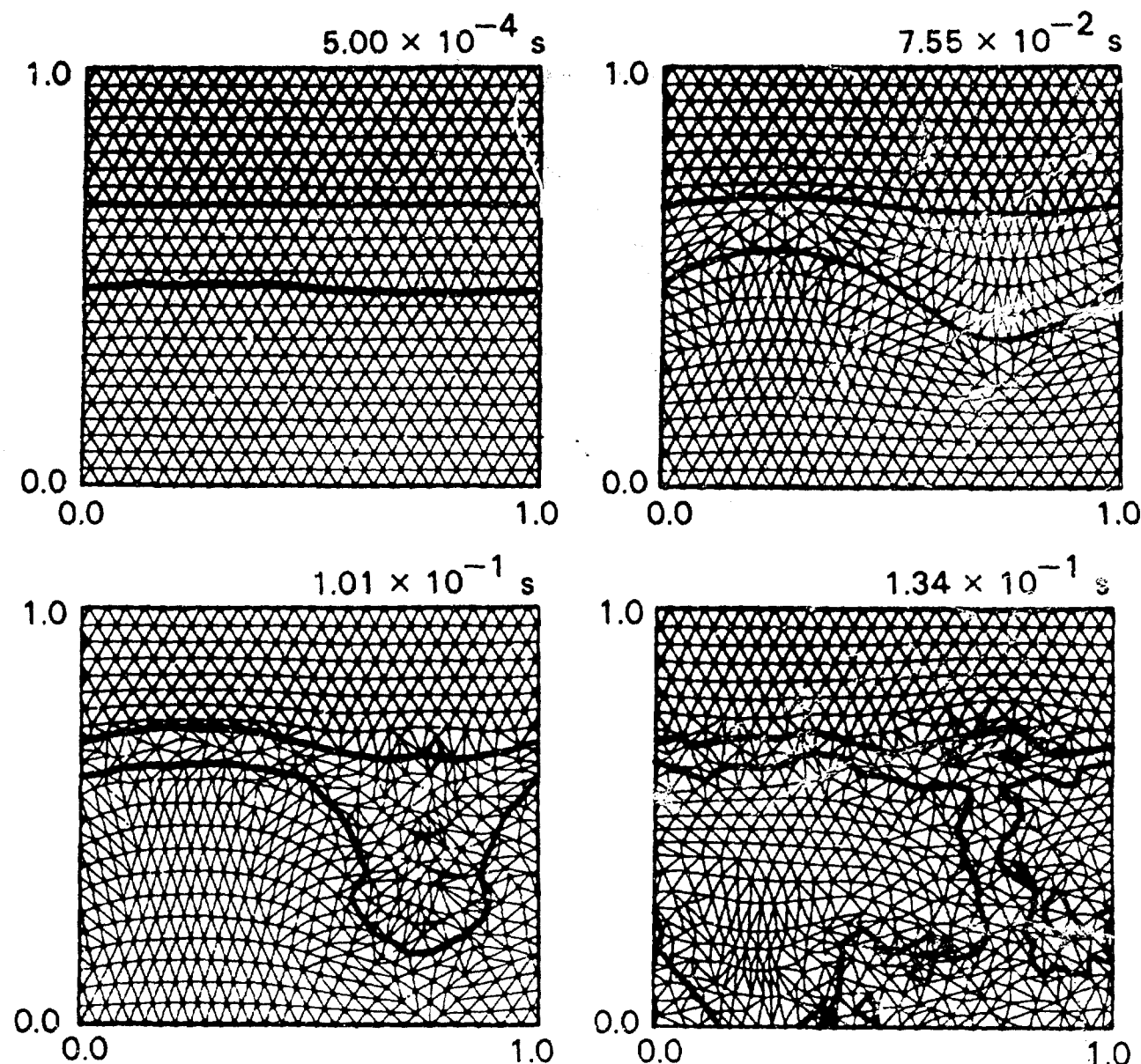


Figure 7. Sequence showing the evolution of a Rayleigh-Taylor instability calculated with a reconnecting Lagrangian grid of triangles. (Figure courtesy of M. Fritts.)

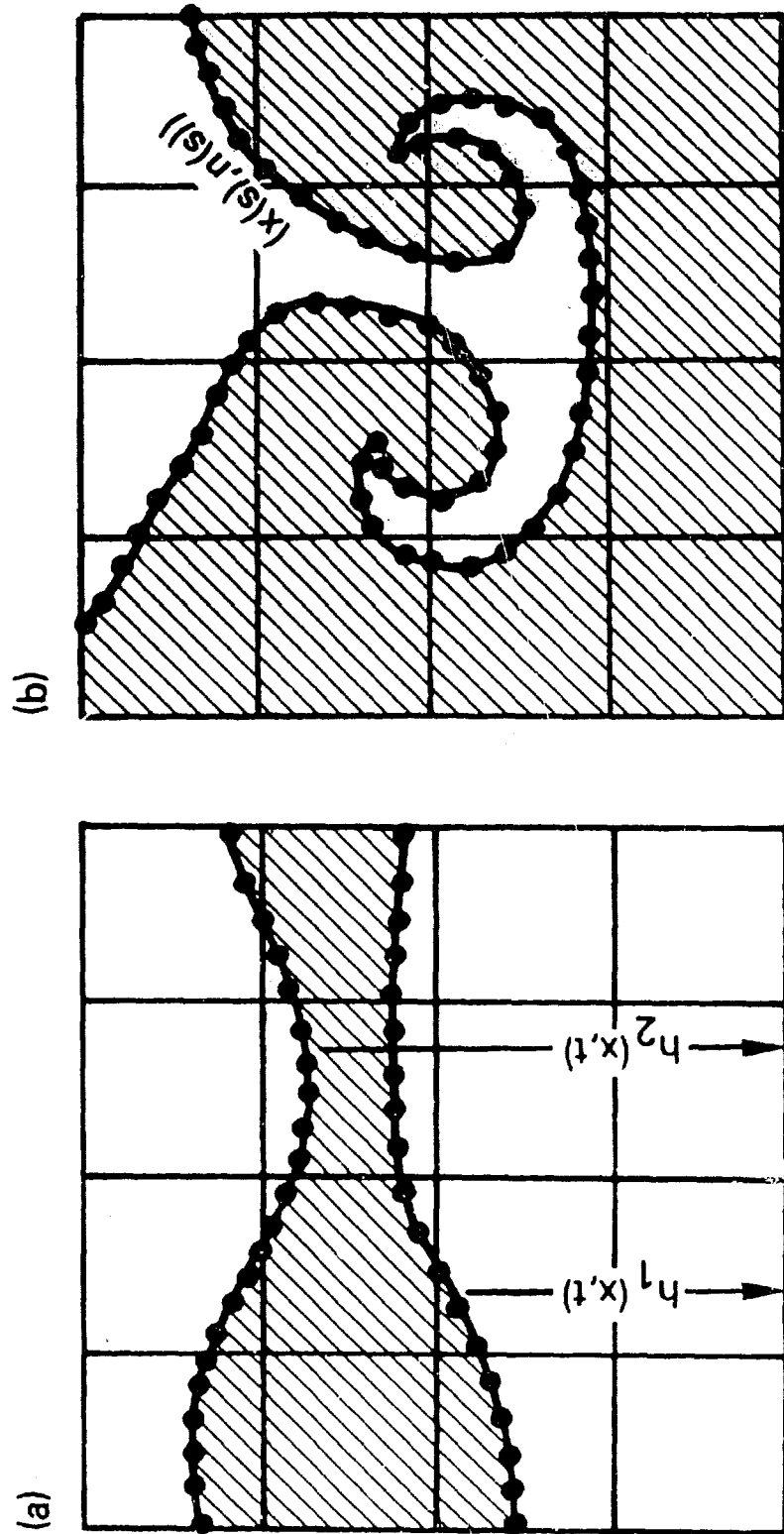


Figure 8. The interface is determined by (a) a sequence of heights above a reference line, or (b) a series of points and a parametric. (Figure courtesy of J.M. Hyman.)

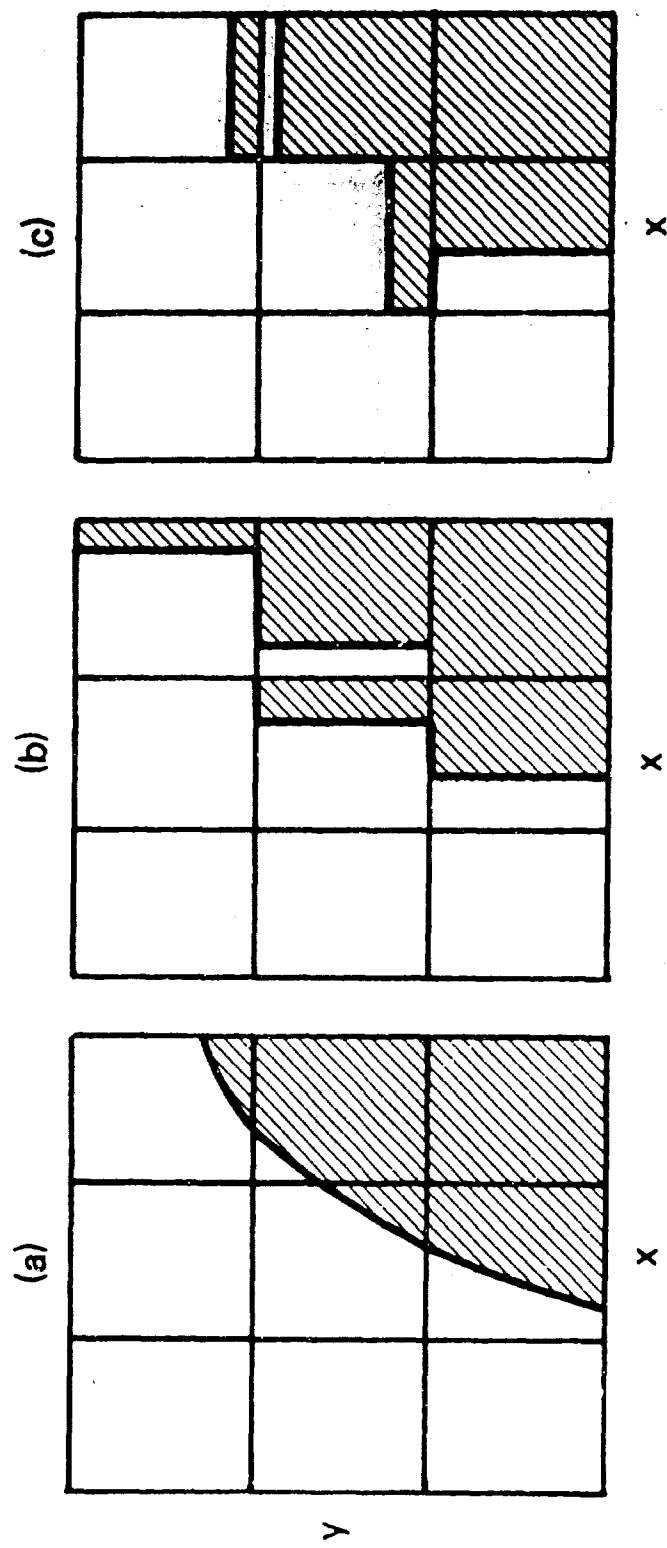


Figure 9. (a) The actual interface. (b) the SLIC representation of it in the  $x$ -pass, and  
 (b) the SLIC representation of it in the  $y$ -pass. (Noh and Woodward, 1976.)

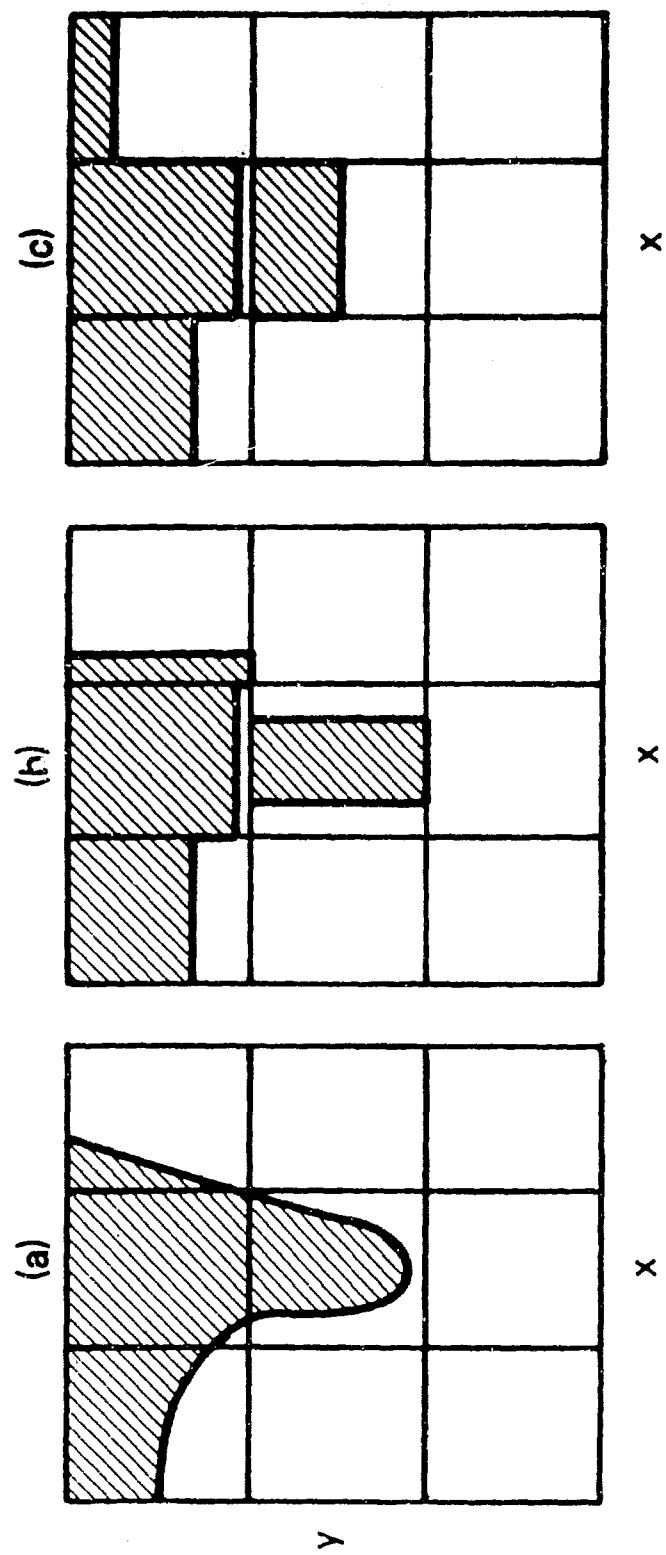


Figure 10. (a) The actual interface. (b) the SLIC representation of it in the  $x$ -pass, and (b) the SLIC representation of it in the  $y$ -pass. (Noh and Woodward, 1976.)

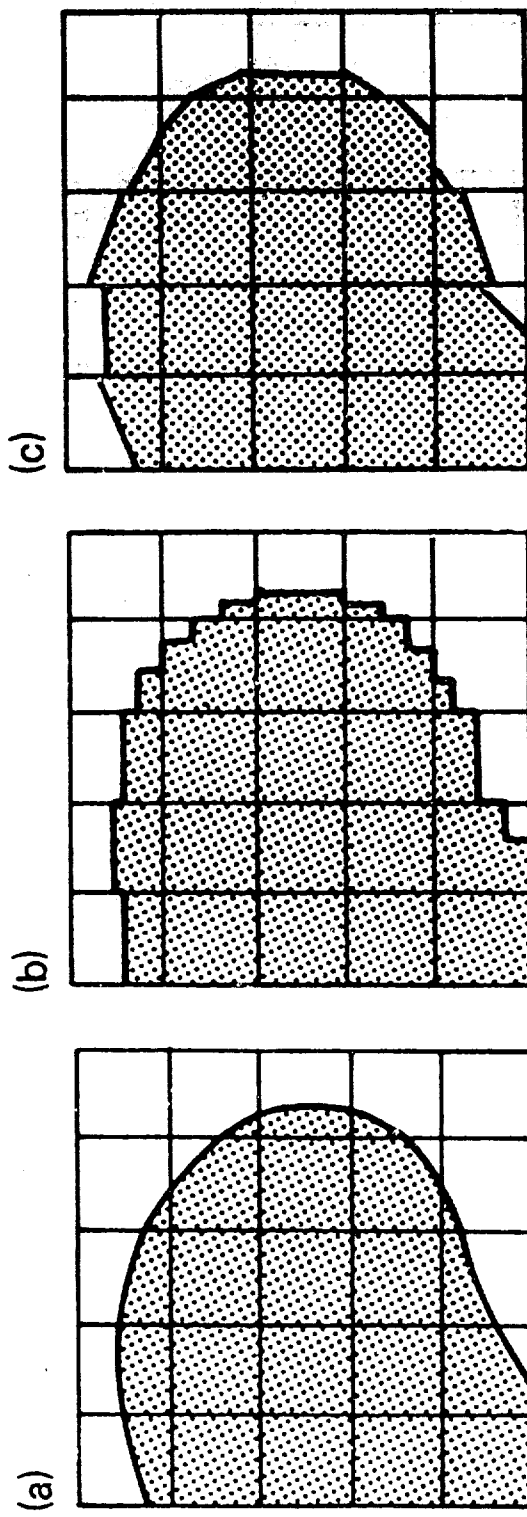


Figure 11. (a) The actual interface. (b) Reconstructed SLIC interfaces for convection.  
 (c) Reconstructed interface for boundary conditions using VOF. (Barr and Ashurst,  
 1984.)

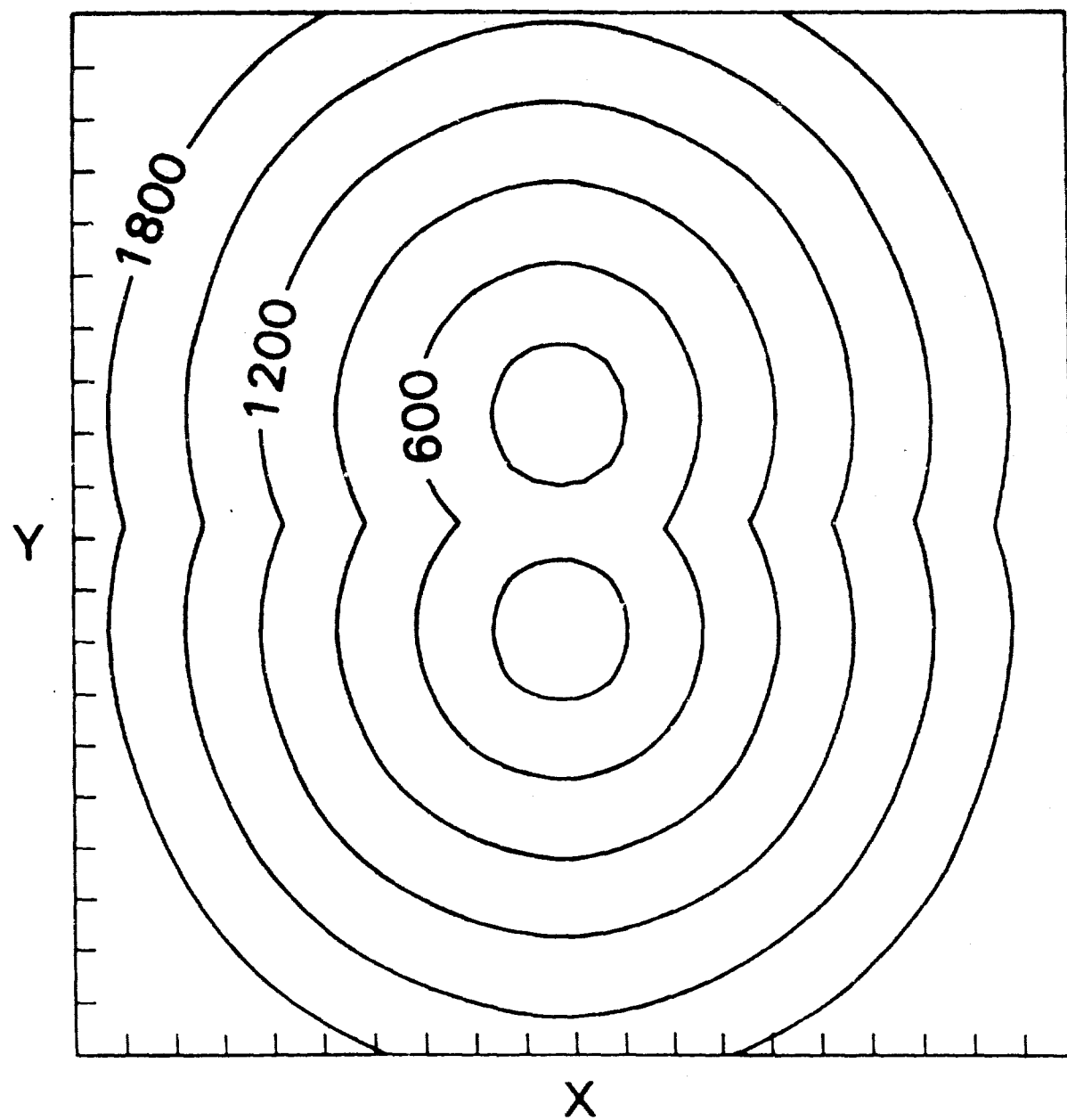


Figure 12. Calculation of two intersecting flame fronts by the gradient method. Successive contours moving out from the center indicate successive times. (Figure courtesy of K. Laskey.)